Available online at **www.joac.info**

ISSN: 2278-1862

Journal of Applicable Chemistry

2018, 7 (4): 973-982

(International Peer Reviewed Journal)

Solution Combustion Route Synthesis of Ag doped $Co_{1-X}Gd_XO$ Nanocomposites and Evaluation of Antibacterial Properties

I.K. Suresh Gowda, H.S. Bhojya Naik*, R. Viswanath and G. Arun Kumar

Department of PG Studies and Research in Industrial Chemistry, School of Chemical Sciences, Kuvempu University, Shankaraghatta-577 451, **INDIA**

Email: hsb_naik@rediffmail.com

Accepted on 5th June, 2018

ABSTRACT

The unique size, composition and morphology dependent properties of nanocomposites are of great interest because they showed promising role in diagnostics and biomedicine. Combustion method has been used as a fast and facile method to prepare Ag doped $Co_{1-X}Gd_XO$ nanocomposite employing glycine as a combustion fuel. The products were characterized by X-ray diffraction technique (XRD), scanning electron microscopy (SEM), transmission electron microscopy (TEM) techniques, and Fourier transformation infrared spectroscopy (FTIR). Experimental results of X-ray diffraction confirmed the formation of CoO phase with spinel Co_3O_4. Transmission electron microscopy indicated that the crystallite size of Ag doped $Co_{1-X}Gd_XO$ nanocomposite was in the range of 5-50 nm. The effect of gadolinium and silver on Co_3O_4 crystallite size and morphology has been discussed. Antibacterial activity of the Ag doped $Co_{1-X}Gd_XO$ nanocomposite was performed using well diffusion method on different pathogens Bacillus subtilis and Klebsiella pneumoniae. These nanocomposites able to resist the growth of bacteria successfully and emerged as a good antibacterial materials.

Graphical Abstract

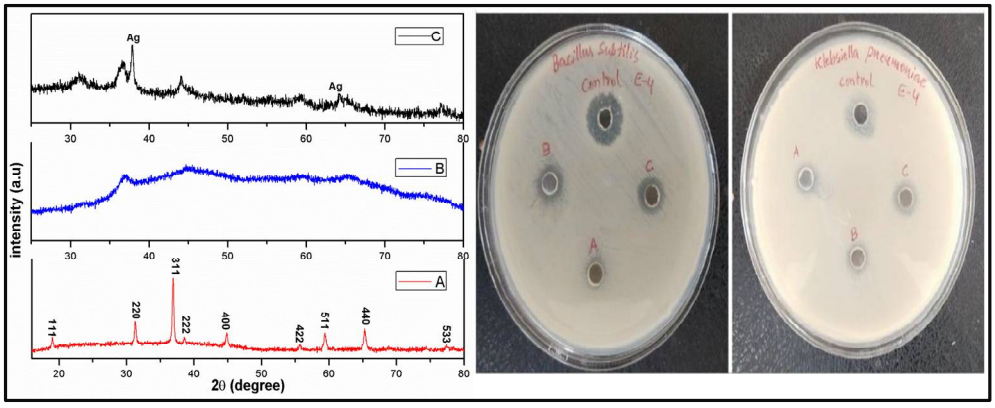

Keywords: Ag doped $Co_{1-X}Gd_XO$ nanocomposite, Solution combustion method, Reactive oxygen species (ROS), Antibacterial activity.

INTRODUCTION

Nanocomposite materials have been widely investigated for the fundamental scientific and technological interests in accessing unique classes of functional materials with extraordinary properties and applications. Due to their small size and morphology, nanoparticles exhibit unique physical, mechanical, chemical, and biological properties that are significantly different from those of their bulk counterparts [1-5]. The nanocomposites have potential practical application in several important technological areas such as drug delivery, bio-imaging, environmental remediation, catalysis, sensors and other electronic devices [6–12].

In recent years, the synthesis of nanosized crystalline metal and metal oxide nanoparticles are of great attraction. Because of their large surface area, surface defects [13], fascinating biological, optical, and chemical properties they have possible applications in many fields including nano-biotechnology [14]. Nanoparticles of metal oxide are extensively being utilized in various industrial products, i.e., catalysts, cosmetics, sun screens and food additives [15-18].

Due to the growing concern of antimicrobial resistance of the pathogens over traditional drugs [19], alternative antimicrobials are needed. Metal nanoparticles have great importance in health and medicine [20]. Potential use of inorganic antimicrobial agents is of great interest because of their advantages over organic antimicrobial agents, because metal and metal oxides possess greater durability, lower toxicity, higher stability and selectivity when compared to traditional organic antimicrobials. Current advances in the field of nanobiotechnology, mainly the ability to prepare metal oxide nanomaterials of definite size, shape, morphology, defects in the crystal structure, monodispersity- providing a rich background for research relevant to the development of new antibacterial agents [21-22].

In vitro and in vivo studies revealed that various metal oxide nanocomposites have potential toxicity effects on pathogens [23–26]. Several metal nanocomposites of two or more metallic components exhibited unique properties like magnetic, electrical, optical and biological activity [27, 28]. Nanocomposites of zinc, cobalt, nickel, silver and iron are being studied extensively as potential antimicrobial agents owing to the beneficial synergistic effects of their components and to discover their enigmatic role in medical nanotechnology [29]. Furthermore, cobalt-based and cobalt oxide nanoparticles, are attracting immense interest owing to their unique structure with excellent size and shape dependent properties such as gas-sensing, catalytic and electrochemical properties and have potential applications in many important fields catalysis, sensors, magnetism, supercapacitors, energy storage, biomedicine etc. [30-32]. It is well known that the morphology and size of nanomaterials have a great influence on its properties, which are thus a key factor to their ultimate performance and applications. In this regard, it is necessary to tailor synthesize nanoparticles with predesigned size and morphology. Furthermore coalescences of metal and metal oxides nanocomposites are expected with high surface area which leads to even more attractive applications in conjunction of their traditional arena and nanotechnology. Therefore, it is important to prepare nanomaterials with defined morphologies and an arrow range of size distribution [33-34].

As the particle size decreases to some extent, a large number of constituting atoms can be found around the surface of the particles, which makes the particles highly reactive with prominent physical properties. It is crucial to control necessary qualities such as size, magnetic behaviour, shape, stability and surface morphology of the particles. Hence manipulation and control of the material properties via mechanistic means is needed [35]. Nanoparticles have been synthesized by various methods like sol–gel, surfactant-mediated synthesis, co-precipitation, hydrothermal synthesis, thermal decomposition and spray-pyrolysis [36-37]. Some of the above methods suffer from the difficulty in size-homogeneity and well dispersion of nanoparticles. In this regard, in our present work we made an attempt to synthesized Ag doped $Co_{1-X}Gd_XO$ nanocomposite by utilizing efficient solution combustion method to evaluate its antibacterial activity.

MATERIALS AND METHODS

Samples of pure Co_3O_4, $Co_{1-X}Gd_XO$ and Ag doped $Co_{1-X}Gd_XO$ were prepared using simple solution combustion method, which allows efficient synthesis of nanosized materials. Glycine acts as a fuel material and metal nitrates were served as oxidiser.

Materials Used: Cobaltnitrate ($Co(NO_3)_2.6H_2O$ -Merck), Gadolinium nitrate ($Gd(NO_3)_3.6H_2O$ -Alfa aesar), Silver nitrate ($AgNO_3$-Alfa aesar) and Glycine($C_2H_5NO_2$-Merck) were of analytical grade reagents and were used as supplied by the commercial supplier without further purification. Distilled water was used as solvent in all of preparations.

(i). Synthesis of Co_3O_4 nanoparticles: The stoichiometric proportions of the cobalt nitrate and glycine were weighed, dissolved in 100 mL distilled water and sonicated for 15 min to get pink coloured clear solution. Then the solution was stirred continuously for 30 min to get homogeneous solution. The obtained sample mixture was then kept in a pre-heated muffle furnace maintained at 400°C. Primarily the gel was formed and the gel gets ignited to give a Co_3O_4 nanoparticles. The samples were washed and dried in an oven at 100°C. The obtained Co_3O_4 nanoparticles were annealed for 2 h maintained at 600°C using muffle furnace.

(ii). Synthesis of $Co_{1-X}Gd_XO$ nanocomposites: In the synthesis of $Co_{1-X}Gd_XO$ nanocomposites, stoichiometric proportions of the cobalt nitrate, gadolinium nitrate and glycine in 100 mL distilled water were weighed and carried out the same procedure similar to the synthesis of Co_3O_4 nanoparticles.

(iii). Synthesis of Ag doped $Co_{1-X}Gd_XO$ nanocomposites: In the synthesis of Ag doped $Co_{1-X}Gd_XO$ nanocomposites stoichiometric proportions of the cobalt nitrate, gadolinium nitrate, silver nitrate (8wt %) and glycine in 100 mL distilled water were weighed and carried out the same procedure similar to the synthesis of Co_3O_4 nanoparticles.

Characterization: Characterization of nanoparticles is necessary to establish the understandings of nature of the material, morphology, their size dependent properties and utilization of these nanocomposites in different applications. Hence the synthesized Co_3O_4, $Co_{1-X}Gd_XO$ and Ag doped $Co_{1-X}Gd_XO$ nanocomposites were characterized through different analytical techniques viz., X-ray diffraction (XRD), Scanning electron microscopy (SEM), High resolution Transmission electron microscopy (HRTEM), Fourier transformation infrared spectroscopy(FTIR), Energy-dispersive X-ray spectroscopy(EDX).

Antibacterial Activity: Antibacterial activity of the Co_3O_4, $Co_{1-X}Gd_XO$ and Ag doped $Co_{1-X}Gd_XO$ nanocomposites was determined using agar disk diffusion method. Antibacterial activity of the as prepared nanocomposites was carried out against two different bacterial strains *B. subtilis*, and *K. pneumoniae*. Bacteria were firstly grown in Müller Hinton broth overnight. 50 µL of the bacterial suspension was thoroughly spread on the nutrient agar plates until plates appeared dry. Then wells were punched into the nutrient agar plates for testing nanomaterial antimicrobial activity. Antibiotic Ampicillin was used as the control. Using a micropipette, about 50 µL of each the Co_3O_4, $Co_{1-X}Gd_XO$ and Ag doped $Co_{1-X}Gd_XO$ nanocomposite suspension and antibiotic solution was then poured on the disks. Plates were incubated at 37°C for 18 h. Antibacterial activity was measured by calculating the diameter of zone of inhibition (ZOI) around the disks.

RESULTS AND DISCUSSION

Morphology and particle size characterization: The XRD studies gives information about the structural and crystallinity of the synthesized nanomaterials. XRD patterns of the Co_3O_4, $Co_{1-X}Gd_XO$

and Ag doped $Co_{1-X}Gd_XO$ nanocomposites calcinated at 600°C, were shown in figure 1, which indicates the cobalt oxide has cubic phase structure.

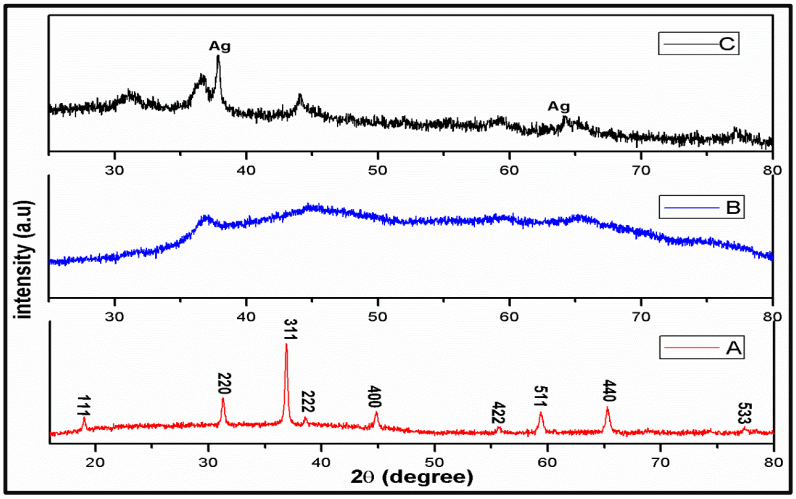

Figure 1: XRD Spectra of (a) Pure Co_3O_4 (b) $Co_{1-X}Gd_XO$ and (c) Ag doped $Co_{1-X}Gd_XO$ nanocomposites.

In figure 1 (a). the diffraction peak positions at 2θ = 19.01°, 31.31°, 36.88°,38.52°,44.87°, 55.78°, 59.36°, 65.26° and 77.41° , associated with the(111), (220), (311),(222), (400), (422), (511), (440) and (533) crystal planes are accounted for the presence of pure cubic Co_3O_4 phase with lattice constant a = 8.084 Å, which is in agreement with the reported value (JCPDS Card No. 80-1545). There were no characteristic peaks of impurity were observed. Thus obtained XRD pattern confirms the formation and purity of pure cubic Co_3O_4 phase. The average crystallite size (D in nm) of nanocomposites were determined from the XRD pattern using the Scherrer's equation i.e.,

$$\mathbf{D = K\lambda / \beta\cos\theta}$$

(where, K is a constant equal to 0.89, λ is the X-ray wavelength equal to 0.154 nm, β is the full width at half maximum and θ is the half diffraction angle) and it was found to be in the range 5-30 nm. In figure 1(b), on addition of gadolinium, due to incorporation of the impurity monoclinic Gd_2O_3 phase, distorted the crystal structure of Co_3O_4 lattice. Since the ionic radii of the Gd^{3+} ion (0.938A˚) is larger than that of the Co^{2+} ion (0.69A˚), the increased concentration of Gd^{3+} ions brought the expansion of crystal lattice. Consequently we can observe that the peaks get broadened invariably and crystallinity of the nanocomposites diminishes and also simultaneously the particle size gets reduced to ~5 nm. In figure 1(c), we observed appearance of peaks at 2θ, 37.85^0 and 64.24^0, these peaks were characteristic peak of cubic metallic silver (JCPDS Card No. 04-0783) which indicates the effective doping and presence of silver in the synthesised nanocomposites and from these XRD pattern we can observe that the diffraction peaks are markedly shifted towards the lower 2θ values and broadened upon the addition of the RE-oxides and silver, thus resulting in the decrease in particle size. The d-spacing value of the crystal planes was found to be 0.23nm.The average crystallite size, d-spacing, strain were calculated and tabulated in table 1.

Figure 2 shows the surface morphology of synthesized nanocomposites at different magnifications. A typical SEM image exhibits non-uniform net like porous nanocomposites with the sizes ranging from 200 to 500 nm. The evolution of gases and release of enormous amount of heat in combustion synthesis method results in the formation of porous nanocomposites and agglomeration of particles due to high temperature, whereas in case of the Ag-doped $Co_{1-X}Gd_XO$ nanocomposites, it showed the change in morphology by the formation of numerous trapped voids

Table 1. Particle size, d-spacing and strain calculated from XRD pattern of Co_3O_4, $Co_{1-X}Gd_XO$ and Ag doped $Co_{1-X}Gd_XO$ nanocomposites.

Sl. No	Sample	Particle Size in nm	d-spacing in A°	Strain x10^{-6}
1	**Pure Co_3O_4**	28.68846295	2.434634460	0.00377647
2	**$Co_{1-X}Gd_XO$**	5.590924423	2.008996116	0.01599067
3	**Ag doped $Co_{1-X}Gd_XO$**	25.8435544	2.374664865	0.00408904

.

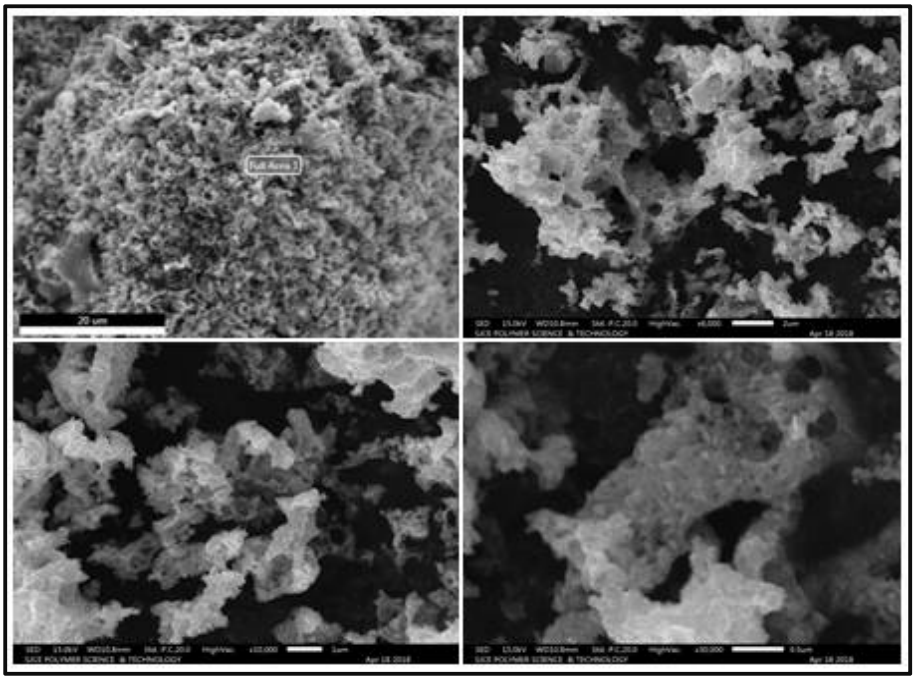

Figure 2. SEM Images of Co_3O_4, $Co_{1-X}Gd_XO$ and Ag doped $Co_{1-X}Gd_XO$ nanocomposites.

The particle surface morphology and also size of the synthesized Ag doped$Co_{1-X}Gd_XO$ nanocomposites were analyzed from TEM images. Figure 3(a) and 3(b) shows the TEM images of the synthesized nanocomposites.

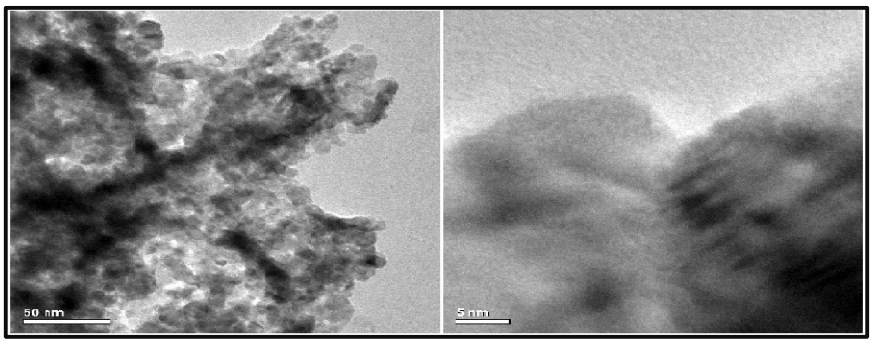

(a) **(b)**

Figure 3. TEM Images of Ag doped $Co_{1-X}Gd_XO$ nanocomposites.

The images revealed that the TEM micrographs of the synthesized Ag doped $Co_{1-X}Gd_XO$ shows polycrystalline nature with uneven shape and slightly agglomerated. The particles size is in the range of 5-50 nm. These results are in a good agreement with the sizes determined from XRD analysis. Moreover, the particles of these nanocomposites have homogeneous and uniform distribution in the powder sample.

Surface modification characterization: The formation and purity of the products were further confirmed by FTIR spectroscopy. FTIR analysis has been carried out to determine the modes of vibrations of chemical bond and surface chemistry present in the prepared samples. FTIR spectra were recorded in solid phase using the KBr pellet technique in the regions of 3500–400 cm^{-1}. Figure 4 shows the FTIR spectra of prepared Ag doped $Co_{1-X}Gd_XO$ nanocomposites.

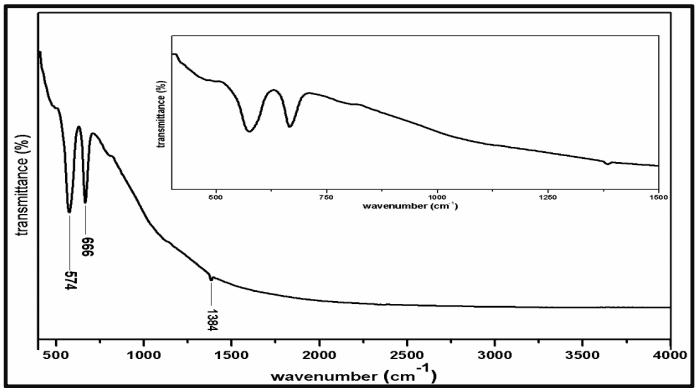

Figure 4. FTIR Spectra of Ag doped $Co_{1-X}Gd_XO$ nanocomposites.

The spectra contained two strong absorption bands at 576 cm^{-1} and 667 cm^{-1} which confirm the spinel structure of Co_3O_4. The band at 576 cm^{-1} can be assigned to the M–O in which M is Co^{+3} and so coordinates octahedral. The peak at 667 cm^{-1} is attributed to the stretching vibration mode of M–O stretching. This confirms the formation of metal oxides [38, 39]. Spectra also contains very weak absorption peak at 1384 cm^{-1} due to metal carbonate structure [40]. And since there was no other absorption peaks in the FTIR it was confirmed that the prepared sample were free of the nitrate-group (2213–2034 cm^{-1}) [41]. These spectra confirm impurity free nanocomposites.

APPLICATION

Antibacterial activity studies: The antibacterial efficacy of pure Co_3O_4, $Co_{1-X}Gd_XO$ and Ag doped $Co_{1-X}Gd_XO$ nanocomposite against gram positive and gram negative pathogens *B. subtilis* and *K. pneumoniae* is shown in figure 5. It can be clearly seen that Ag doped $Co_{1-X}Gd_XO$ nanocomposites

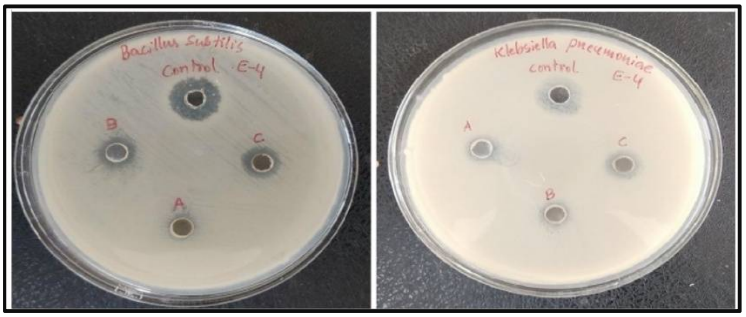

Figure 5. Antibacterial activity of (A) Pure Co_3O_4 (B) $Co_{1-X}Gd_XO$ and (C) Ag doped $Co_{1-X}Gd_XO$ nanocomposites and control (Ampicillin) against (a) *Bacillus subtilis* and (b) *Klebsiella pneumoniae*.

has exhibited better antibacterial efficiency on both the gram positive gram negative pathogens. Furthermore we observed that the $Co_{1-X}Gd_XO$ nanocomposite showed nearly same antibacterial efficiency compared to Ag doped $Co_{1-X}Gd_XO$ nanocomposite. Because of very small crystallite size (~5nm) $Co_{1-X}Gd_XO$ nanocomposite even though in the absence of Ag dopant, due to high surface ions there is an effective interaction with the cell wall and showed better antibacterial activity. These results confirm that antibacterial activity not only depends on composition it also depends on size and morphology.

Smaller nanoparticles exhibit greater toxicity. Smaller the size of the nanocomposites higher will be the zone of inhibition, since it facilitates the nanocomposites to passivate through the cell wall of the bacteria resulting in formation of reactive oxygen species (ROS) which is responsible for cell death.The zones of inhibition of synthesized nanocomposites were tabulated in table 2.

Table 2: Zone of inhibition in millimetre (mm) of Pure Co_3O_4, $Co_{1-X}Gd_XO$ and Ag doped $Co_{1-X}Gd_XO$ nanocomposites against (a) Bacillus subtilis and (b) Klebsiella pneumoniae.

Name of The Compound	Concentration	Organism Used	Zone of Inhibition (mm)
Co_3O_4 (E 4 - A)	50µg 50µL^{-1}	*B.Subtilis*	10±1.5
		K.pneumoniae	10±0.9
$Co_{1-X}Gd_XO$ (E 4 – B)	50µg 50µL^{-1}	*B.Subtilis*	13±0.8
		K.pneumoniae	12±0.4
Ag doped $Co_{1-X}Gd_XO$ (E 4 – C)	50µg 50µL^{-1}	*B.Subtilis*	13±1.1
		K.pneumoniae	12±1.8
Control (Ampicillin)	50µg 50µl^{-1}	*B.Subtilis*	17±0.4
		K.pneumoniae	17±0.3

The highest antibacterial activity of Ag doped $Co_{1-X}Gd_XO$ nanocomposite was observed against *B. subtilis* (ZOI-13±1.1). Therefore, based on these results it can be suggested that Ag doped $Co_{1-X}Gd_XO$ nanocomposite can be a good antibacterial agent.

CONCLUSIONS

The nanosized particles of pure Co_3O_4, $Co_{1-X}Gd_XO$ and Ag doped $Co_{1-X}Gd_XO$bnanocomposite were synthesized by the solution combustion method. XRD and TEM results showed that Ag doped $Co_{1-X}Gd_XO$nanocompositewere polycrystalline in nature and ultra small in size ranging from 5-50 nm. SEM images showed the net like porous nanocomposites with numerous trapped voids. FTIR studies confirmed the formation of metal oxides. Furthermore, the antibacterial activity of all the three synthesized nanocomposites was studied against bacteria *Bacillus subtilis* and *Klebsiella pneumonia*. Ag doped $Co_{1-X}Gd_XO$ nanocomposite showed excellent bactericidal potential with highest zone of inhibition (13±1.1mm) against gram positive bacteria *B. Subtilis* compared to other nanocomposites. Antibacterial activity increased with decrease in particle size, as the formation of ROS by the effective interaction of nanocomposites with bacteria. It will be of great interest for the future studies to find the antibacterial potential of Ag doped $Co_{1-X}Gd_XO$ nanocomposite against antibiotic resistant bacteria and to evaluate antitumor activity as well.

ACKNOWLEDGEMENTS

The authors gratefully acknowledge Department of Industrial Chemistry, Kuvempu University, for providing lab facilities.

.

REFERENCES

[1]. Alex, Saji, Tiwari, Ashutosh, Functionalized Gold Nanoparticles: Synthesis, Properties and Applications-A Review, *Journal of Nanoscience and Nanotechnology*, **2015**, 15(26), 1869-1894.

[2]. Maria-Eleni Kyriazi, Otto L. Muskens, Antonios G. Kanaras, "Functionalized nanoparticles and applications", *Proc. SPIE*, Colloidal Nanoparticles for Biomedical Applications XII, **2017**, 10078; doi: 10.1117/12.2245441.

[3]. K. Lu, Nanocrystalline metals crystallized from amorphous solids: nanocrystallization, structure, and properties, *Mater. Sci. Eng. R. Rep*.**1996**, 16, 161-221.

[4]. N. R. Tao, Z. B. Wang, W. P. Tong, M. L. Sui, J. Lu, K. Lu, An investigation of surface nanocrystallization mechanism in Fe induced by surface mechanical attrition treatment, *Acta Mater.*, **2002**, 50, 4603-4616.

[5]. A Stanković, S Dimitrijević, D Uskoković, Influence of size scale and morphology on antibacterial properties of ZnO powders hydrothemally synthesized using different surface stabilizing agents, *Colloids and Surfaces B: Biointerfaces*, **2013**, 102, 21-28.

[6]. J. Li, X. Shi, M. Shen , Hydrothermal synthesis and functionalization of iron Oxide Nanoparticles for MR Imaging Applications, *Part. Part. Syst. Charact*., **2014**, 31, 1223.

[7]. Guilong Zhang, Ruohong Du, Lele Zhang, Dongqing Cai, Xiao Sun , Yong Zhou, Jian Zhou, Junchao Qian , Kai Zhong, Kang Zheng, Darnell Kaigler, Wenqing Liu, Xin Zhang, Duohong Zou, Zhengyan Wu, Gadolinium-Doped Iron Oxide Nanoprobe as Multifunctional Bioimaging Agent and Drug Delivery System, *Adv. Funct. Mater*., **2015**, 25, 6101–6111.

[8]. A. H. Lu, E. L. Salabas, F. Schüth, Magnetic nanoparticles: synthesis, protection, functionalization and application, *Angew Chem.Int. Ed Engl*., **2007**, 46, 1222–1244.

[9]. H. Heli, J.Pishahangd, Cobalt oxide nanoparticles anchored to multiwalled carbon nanotubes: Synthesis and application for enhanced electrocatalytic reaction and highly sensitive nonenzymatic detection of hydrogen peroxide, *Electrochimica Acta*. **2014**, 123, 518-526.

[10]. Xiliang Luo, Aoife Morrin, Anthony J. Killard, Malcolm R. Smyth, Application of Nanoparticles in Electrochemical Sensors and Biosensors, *Electroanalysis*. **2006**, 18, 319-326.

[11]. Edson R. Leite, Ingrid T. Weber, Elson Longo, and Jose A. Varela, A New Method to Control Particle Size and Particle Size Distribution of SnO_2 Nanoparticles for Gas Sensor Applications, *Adv. Mater*., **2000**, 12, 965-968.

[12]. A. B. Djurisic, A. M. C. Ng, X. Y. Chen, ZnO nanostructures for optoelectronics: Material properties and device applications, *Progress in Quantum Electronics*, **2010**, 34, 191-259.

[13]. S. J. Zinkle, K. Farrell, Void swelling and defect cluster formation in reactor irradiated copper, *J. Nucl. Mater*., **1989**, 168, 262-267.

[14]. S. Khan, A. A Ansari, A. A Khan, R Ahmad, O Al-Obaid, W Al-Kattan, "In vitro evaluation of anticancer and antibacterial activities of cobalt oxide nanoparticles," *J Biol Inorg Chem*., **2015**, 20, 1319-1326.

[15]. J. Jang, J.H. Oh, Fabrication of a Highly Transparent Conductive Thin Film from Polypyrrole/Poly (methyl methacrylate) Core/Shell Nanospheres, *Adv. Func. Mater*. , **2005**, 15, 494.

[16]. C. E. Small, S. Chen, J. Subbiah, C .M. Amb, S.W. Tsang, T. H. Lai, J. R. Reynolds, F. So, High-efficiency inverted dithienogermole–thienopyrrolodione-based polymer solar cells, *Nat. Phot*., **2012**, 6, 115.

[17]. G.J. Nohynek, J, Lademann, C. Ribaud, M. S. Roberts. Grey goo on the skin? Nanotechnology, cosmetic and sunscreen safety, *Crit Rev Toxicol*., **2007**, 37, 251-77.

[18]. K. Blecher, A. Nasir, A. Friedman, The growing role of nanotechnology in combating infectious disease, *Virulence*, **2011**, 2, 395-401.

[19]. N. Yael. Slavin, Jason Asnis, O. Urs. Häfeli, Horacio Bach, Metal nanoparticles: understanding the mechanisms behind antibacterial activity, *J Nanobiotechnol*., **2017**, 15, 65.

[20]. Y. Liu, L. He, A. Mustapha, H. Li, Z. Q. Hu, M. Lin, Antibacterial activities of zinc nanoparticles against Escherichia coli, *J. Appl. Microbiol*., **2009**, 107, 1193-1201.

[21]. H. Shi, R. Magaye, V. Castranova, J. Zhao, Titanium dioxide nanoparticles: a review of current toxicological data, *Part Fibre Toxicol.,* **2013**, 10,15.
[22]. Slavica Stankic, Sneha Suman, Francia Haque, Jasmina Vidic, Pure and multi metal oxide nanoparticles: synthesis, antibacterial and cytotoxic properties, *J. Nanobiotechnol.*, **2016**, 14, 73.
[23]. Leanne M. Gilbertson, Eva M. Albalghiti, Zachary S. Fishman, François Perreault, Charlie Corredor, Jonathan D. Posner, Menachem Elimelech, Lisa D. Pfefferle, Julie B. Zimmerman, Shape-Dependent Surface Reactivity and Antimicrobial Activity of Nano-Cupric Oxide, *Environ. Sci. Technol*., **2016**, 50, 3975-3984.
[24]. Shahanavaj Khan, Anees A. Ansari, Abdul Arif Khan, Rehan Ahmad, Omar Al-Obaid, Wael Al-Kattan, In vitro evaluation of anticancer and antibacterial activities of cobalt oxide nanoparticles, *J Biol Inorg Chem*., **2015**, 20, 1319–1326.
[25]. S. Chattopadhyay, S. P. Chakraborty, D. Laha, R. Baral, P. Pramanik, S. Roy, Surface-modified cobalt oxide nanoparticles: new opportunities for anti-cancer drug development, *Cancer Nano.*, **2012**, 3,13-23
[26]. [26]. R. S. Kumaran, Y. K. Choi, V Singh, H. J. Song, K. G. Song, K. J. Kim, H. J. Kim, In vitro cytotoxic evaluation of MgO nanoparticles and their effect on the expression of ROS genes, *Int. J. Mol. Sci.*, **2015**, 16, 7551-7564.
[27]. Y. Mao, T. J. Park, S. S. Wong, Synthesis of classes of ternary metal oxide nanostructures, *Chem Commun*., **2005**, 46, 5721-35.
[28]. Igor Shmarakov, Iuliia Mukha, Nadiia Vityuk, Vira Borschovetska, Nelya Zhyshchynska, Galyna Grodzyuk, Anna Eremenko, Antitumor Activity of Alloy and Core-Shell-Type Bimetallic AgAu Nanoparticles, *Nanoscale Research Letters,* **2017,** 12**,** 333.
[29]. YW Jun, JH Lee, J Cheon, Chemical design of nanoparticle probes for high-performance magnetic resonance imaging, *Angew Chem Int Ed Engl.*, **2008**, 47, 5122–5135.
[30]. Faranak Manteghi, Sayed Habib Kazemi, Masoud Peyvandipour, Ahmad Asghari, Preparation and Application of Cobalt Oxide Nanostructures as Electrode Materials for Electrochemical Supercapacitors, *RSC Adv.*, **2015**, 5, 76458.
[31]. Naoto Koshizaki, Katsuya Yasumoto, TakeshiSasaki, A gas-sensing CoO/SiO2 Nanocomposite, *Nanostructed Materials*. **1999**, 12, 971–74.
[32]. Q. A.Pankhurst, J. Connolly, S. K. Jones, J. Dobson, Applications of magnetic nanoparticles in biomedicine, *Journal of Physics D: Applied Physics*, **2003**, 36, R167-R181.
[33]. A. Azam, A. S. Ahmed, M. Oves, M. S. Khan, A. Memic, Size-dependent antimicrobial properties of CuO nanoparticles against Gram-positive and -negative bacterial strains, *Int J Nanomedicine*, **2012**, 7, 3527-3535.
[34]. Y. Pan, S. Neuss, A. Leifert, M. Fischler, F. Wen, U. Simon, G. Schmid, W. Brandau, W. Jahnen-Dechent, Size dependent cytotoxicity of gold nanoparticles, *Small*. **2007**, 3, 1941-9.
[35]. Mohammad Vaseem, Ahmad Umar, Yoon-Bong Hahn, ZnO Nanoparticles: Growth, Properties, and Applications, *Materials and Devices,* **2010**, 5, 1-36.
[36]. Y. Roh, H. Vali, T. J. Phelps, JW Moon, Extracellular synthesis of magnetite and metal-substituted magnetite nanoparticles, *J. Nanosci Nanotechnol*., **2006**, 6, 3517-3520.
[37]. A. A. Bharde, R. Y. Parikh, M. Baidakova, S. Jouen, B. Hannoyer, T. Enoki, B. L. Prasad , Y. S. Shouche, S. Ogale, M. Sastry, Bacteria-mediated precursor-dependent biosynthesis of superparamagnetic iron oxide and iron sulfide nanoparticles, *Langmuir*. **2008**, 24, 5787-5794.
[38]. M. Salavati-Niasari, F. Davar, M. Mazaheri, M. Shaterian, Preparation of cobalt nanoparticles from [bis(salicylidene)cobalt(II)]–oleylamine complex by thermal decomposition, *J. Magn. Magn. Mater*., **2008**, 320, 575-578.
[39]. M. Herrero, P. Benito, F. M. Labajos, V. Rives, Nanosize cobalt oxide-containing catalysts obtained through microwave-assisted methods, *Catal. Today*, **2007**, 128, 129.
[40]. Beatriz Cela, Daniel A.de Macedo, Graziele L.de Souza, AntonioE.Martinelli, Rubens M.do Nascimento, Carlos A. Paskocimas, NiO–CGO in situ nanocomposite attainment: One step synthesis, *Journal of Power Sources*, **2011**, 196, 2539-2544.

[41]. N. Dhananjaya, H. Nagabhushana, B.M. Nagabhushana, B. Rudraswamy, S.C. Sharma, D.V. Sunitha, C. Shivakumara, R.P.S. Chakradhar, Effect of different fuels on structural, thermo and photoluminescent properties of Gd_2O_3 nanoparticles, *Spectrochimica Acta Part A: Molecular and Biomolecular Spectroscopy*, **2012**, 96, 532–540.